

## The constructal law origin of the logistics S curve

A. Bejan<sup>1</sup> and S. Lorente<sup>2</sup>

<sup>1</sup>*Department of Mechanical Engineering and Materials Science, Duke University, Durham, North Carolina 27708-0300, USA*

<sup>2</sup>*Université de Toulouse, INSA, Laboratoire Matériaux et Durabilité des Constructions (LMDC), 135, Avenue de Rangueil, F-31 077 Toulouse Cedex 04, France*

(Received 2 May 2011; accepted 28 May 2011; published online 20 July 2011)

The S curve is one of the most common phenomena in nature: the spreading of populations, tumors, contaminants, innovations, economic activity. Here we show that this phenomenon can be predicted entirely by recognizing in it a flow. The flow is not by diffusion alone, rather it is a combination of tree-shaped “invasion” by convection, followed by “consolidation” by diffusion perpendicular to the invasive lines. The S curve is not unique: its scales depend on the relative magnitude of the speed of the invading lines and the diffusivity perpendicular to the lines. Tree-shaped invasion covers the territory with diffusion much faster than line-shaped invasion. The predicted S-curve flow architecture unites the designs of spreading flows and collecting flows (e.g., mining, fossil fuel extraction, Hubbert peak) in all the realms of nature: animate, inanimate, and human-made. © 2011 American Institute of Physics. [doi:10.1063/1.3606555]

### I. SPREADING FROM POINT TO AREA OR VOLUME

When something spreads on a territory, the curve of territory size versus time is S-shaped: slow initial growth is followed by much faster growth, and finally by slow growth again. The corresponding curve of the rate of spreadings versus time is bell shaped. This phenomenon is so common<sup>1-3</sup> (Fig. 1) that it has generated entire fields of research that seem unrelated: the spreading of biological populations, tumors, chemical reactions, contaminants, languages, news, information, innovations, technologies, infrastructure, and economic activity.<sup>4-8</sup>

The natural phenomenon is not a particular mathematical expression for the S-shaped curve (in fact, in this paper we will show that the S-shaped curves are not unique). The natural phenomenon is the very frequent observation that in many flow systems (e.g., Fig. 1) the covered territory increases in time according to a curve that resembles an S.

The prevalence of S-curve phenomena in nature rivals that of tree-shaped flows, which also cover the animate, inanimate, and human realms. Here we show that this is not a coincidence. Both phenomena are manifestations of the natural tendency of flow systems to generate evolving designs that allow them to flow, spread, and collect more easily.<sup>9,10</sup> This tendency is summarized by the constructal law: “For a finite-size flow system to persist in time (to live), its configuration must evolve such that it provides easier and easier access to its currents.”<sup>3,11</sup> A growing volume of research is showing that the constructal law accounts for phenomena of design and evolution across the board, animate and inanimate, from physics to biology and social organization.<sup>9-20</sup>

### II. LINE-SHAPED INVASION AND CONSOLIDATION

S-curve observations are often called “diffusion” of change, innovation, technology, infrastructure, etc. Here we point out that diffusion alone cannot account for the S shape. For example, if matter or energy were to diffuse from one

boundary point into an area, the radius of the patch swept by diffusion would increase as  $(\alpha t)^{1/2}$ , where  $\alpha$  (m<sup>2</sup>/s) is the diffusivity (mass, heat) relative to the medium that occupies the area, and  $t$  is the time.<sup>21</sup> The diffused area would grow as the radius squared (i.e., as  $t$ ), and the curve would be a straight line, not an S.

From turbulence and river basins to human lungs, natural flow structures do not flow by diffusion alone.<sup>9-11</sup> They combine two flow mechanisms (convection and diffusion) in order to facilitate the flow over the entire available space. Figure 2 shows how. Mass or energy spreads from point to area in two successive phases. First, it *invades* the available area  $(2L_1)^2$  with the speed  $V$  along the channel  $L = Vt$  during the time  $t_{in} = 2L_1/V$ , while diffusion spreads transversally, on both sides of  $L$ .

The following analysis is presented in terms of convective versus conductive heat transfer, although similar two-mechanism analyses can be formulated for each of the flow architectures that exhibit the  $S(t)$  curve while spreading or collecting.

The invading line has a constant temperature  $(T_0 + \Delta T)$ , which is different than the initial temperature of the invaded medium  $(T_0)$ . In the vicinity of the invading line the thickness scale ( $\delta$ ) of the diffused area is such that the transversal diffusion time ( $\delta^2/\alpha$ ) is the same as the time of longitudinal advance  $(L/V)$ . From this follows  $\delta \sim (\alpha L/V)^{1/2}$  and the finger-shaped area covered by diffusion  $\delta L \sim \alpha^{1/2} V t^{3/2}$ . At the end of invasion ( $t_{in}$ ), the diffused area has grown to  $A_{in} \sim \alpha^{1/2} V^{-1/2} (2L_1)^{3/2}$ ,

$$\frac{A}{A_{in}} \sim \left( \frac{t}{t_{in}} \right)^{3/2}. \quad (1)$$

Equation (1) accounts for the early part of the S curve, because  $dA/dt$  increases monotonically.

After  $t_{in}$ , the available area is filled by diffusion above and below the finger of length  $2L_1$ . This is the *consolidation*

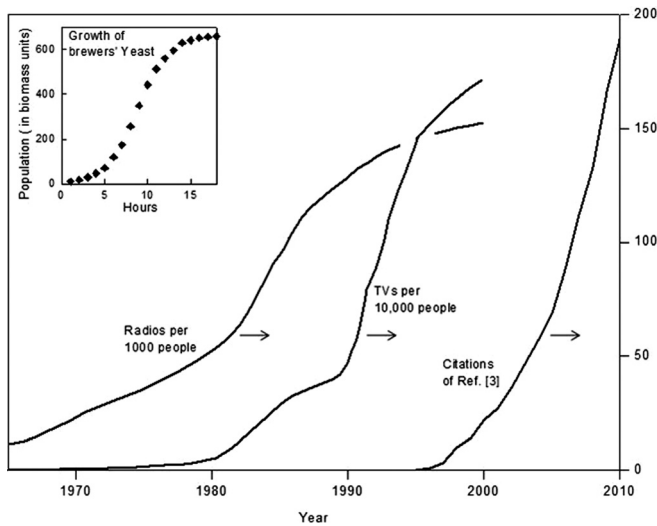


FIG. 1. Examples of S-curve phenomena: the growth of brewer’s yeast (Ref. 1), the spreading of radios and TVs (Ref. 2), and the growth of the readership of scientific publications (Ref. 3).

phase, and it lasts until  $t_{co} \sim L_1^2/\alpha$ . The thickness of the area covered by diffusion is  $(\alpha t)^{1/2}$ . The area swept by diffusion is  $A_{co} \sim 2 \times (2L_1) \times (\alpha t)^{1/2}$ , and its history is

$$\frac{A}{4L_1^2} \sim \left(\frac{t}{t_{co}}\right)^{1/2}. \quad (2)$$

This accounts for the late part of the S curve, because  $dA/dt$  decreases monotonically.

The scales of the invasion and consolidation periods depend on the invasion speed and diffusivity:

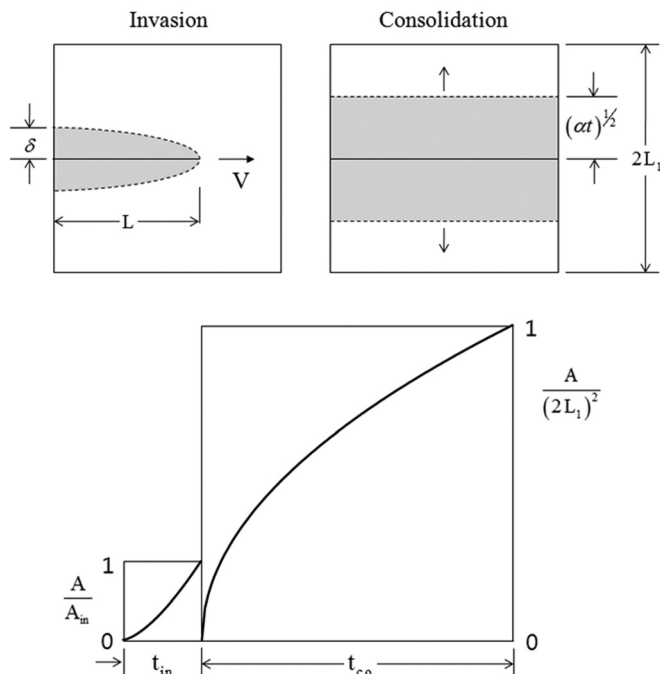


FIG. 2. Line-shaped invasion, followed by consolidation by transversal diffusion. The predicted history of the area covered by diffusion reveals the S-shape curve.

$$\frac{t_{co}}{t_{in}} \sim \frac{L_1 V}{2\alpha} > 1, \quad (3)$$

$$\frac{A_{in}}{4L_1^2} \sim \left(\frac{\alpha}{2L_1 V}\right)^{1/2} < 1. \quad (4)$$

The group  $L_1 V/\alpha$  must be greater than 1, because the invasion finger must be slender.

In summary, the invasion-consolidation analysis accounts for the S curve entirely. It also predicts that the S shape is not unique, because it depends on the group  $L_1 V/\alpha$ . Because the point-area spreading is natural, it has the tendency and freedom to generate configurations that allow it to cover the available area during a time shorter than  $t_{co} \sim L_1^2/\alpha$ . We show next that the configuration that offers greater access than the line invasion is a tree-shaped invasion.

### III. TREE-SHAPED INVASION AND CONSOLIDATION

Figure 3 shows a tree of mass or energy supply that emerges from the side, and grows at constant speed  $V$ . We continue to model this invading tree in heat transfer terms, as lines with a temperature that differs from the ambient temperature. The first line is the trunk of the growing tree. When it reaches the center, it bifurcates and continues to invade at constant speed. Bifurcations occur in the sequence  $L_1, L_2 = (\frac{1}{2})L_1, L_3 = (\frac{1}{2})L_1$ , etc. approximately

$$L_{i+1}/L_i = 2^{-1/2}. \quad (5)$$

Diffusion spreads laterally from every invading line. The thickness ( $\delta_i$ ) of each diffused area is thin in comparison with the length ( $L_i$ ),  $\delta_i < L_i$ , therefore

$$\left(\frac{L_i V}{\alpha}\right)^{1/2} > 1. \quad (6)$$

In time, this condition breaks down as the branches ( $L_i$ ) become so small that their boundary areas ( $\delta_i L_i$ ) are no longer slender ( $\delta_i \sim L_i$ ). The smallest branches ( $i = n$ ) mark the end of the invasion phase,

$$\left(\frac{L_n V}{\alpha}\right)^{1/2} \sim 1. \quad (7)$$

This is the start of the consolidation phase: the smallest interstices ( $\delta_n L_n \sim L_n^2$ ) are swept by diffusion over the length scale  $L_n$ .

Measured from the tree root to the tip of any of the smallest branches, the length traveled by each of the  $V$  tips of the invading branches is

$$\begin{aligned} L_{in} &= L_1 + L_2 + L_3 + \dots + L_n \\ &= L_1 \frac{1 - (2^{-1/2})^{n+1}}{1 - 2^{-1/2}}. \end{aligned} \quad (8)$$

When  $n \gg 1$ ,  $L_{in} = 3.4 L_1$  and the total invasion time is  $t_{in} = 3.4 L_1/V$ .

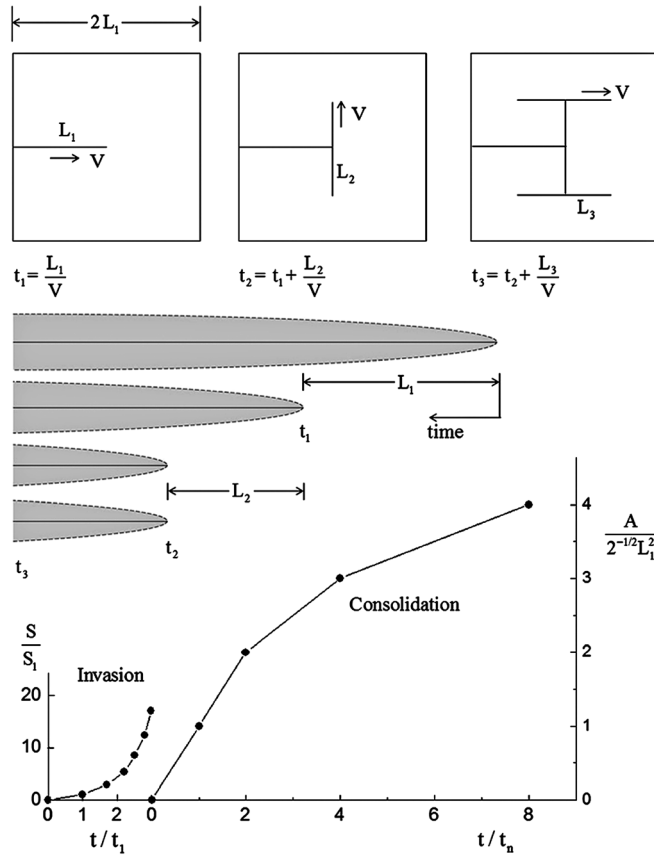


FIG. 3. Tree-shaped invasion, showing the narrow regions covered by diffusion in the immediate vicinity of the invasion lines.

Figure 3 is a rectilinear summary of the growth of the diffused area around the invading tree. At every branching moment, the number of branches doubles and the branch lengths are sized according to Eq. (5). Because the tip speed  $V$  is constant, the abscissa of Fig. 3 also indicates the age of the tree structure. All the diffused regions have the same rounded nose shape (Fig. 3), because all the tips advance with the same speed. The older regions are long, and the younger are short. The most recent finger regions are just barely slender.

The calculation of the diffused area during invasion is illustrated in Fig. 3. First is the slender region  $S_1$  of the initial intrusion of length  $L_1$  at  $t_1 \sim L_1/V$ ,

$$S_1 \sim \delta_1 L_1 \sim \left(\frac{\alpha}{V}\right)^{1/2} L_1^{3/2}. \quad (9)$$

At the next branching,  $t_2 \sim (L_1 + L_2)/V$ , there is a new finger region  $L_2$  and the diffused area

$$S_2 \sim \left(\frac{\alpha}{V}\right)^{1/2} (L_1 + L_2)^{3/2} + \left(\frac{\alpha}{V}\right)^{1/2} L_2^{3/2}, \quad (10)$$

or  $S_2/S_1 \cong 2.83$ . The diffused areas  $S_i$  at subsequent bifurcation times [ $t_i = (L_1 + \dots + L_i)/V$ ] are calculated similarly. They reveal a string of points that could be approximated (fitted) with a curve with increasing  $dA/dt$ , which resembles the short-times portion of observed logistics S curves. This is analogous to the invasion phase ( $0 < t < t_{in}$ ) of the line-shaped invasion in Fig. 2.

Invasion ends at  $t_{in}/t_1 \sim 3.4$ , when the diffused area is of order  $S_{in}/S_1 \sim 30$ . Compared with the area of the square  $(2L_1)^2$ , this area represents the fraction

$$\frac{S_{in}}{4L_1^2} \sim 7.5 \left(\frac{\alpha}{L_1 V}\right)^{1/2}. \quad (11)$$

After  $t \sim t_{in}$ , branches smaller than  $L_n$  cannot grow because diffusion perpendicular to every  $L_n$  line is the flow for covering the smallest interstices [ $L_n L_{n-1}$ , where  $L_n \sim (2^{-1/2})^{n-1} L_1$ ]. There are  $2^{n-1}$  such interstices, and their combined area and sweep time are

$$A_n \sim 2^{n-1} L_n^2 \sim L_1^2, \quad (12)$$

$$t_n \sim \frac{L_n^2}{\alpha} \sim 2^{-(n-1)} \frac{L_1^2}{\alpha}. \quad (13)$$

The next interstices that are swept are larger, of area  $L_n L_{n-1}$  dictated by the length of the branch  $L_{n-1}$  and the perpendicular distance to the next smaller branch ( $L_n$ ) that serves as cut-off for diffusion perpendicular to  $L_{n-1}$ . There are  $2^{n-2}$  interstices of size  $L_n L_{n-1}$  and their combined area and sweep time are

$$A_{n-1} \sim 2^{n-2} L_n L_{n-1} \sim 2^{-1/2} L_1^2 \sim A_n, \quad (14)$$

$$t_{n-1} \sim \frac{L_n^2}{\alpha} \sim t_n. \quad (15)$$

A pattern develops beginning with the next cumulative area, which consists of  $2^{n-3}$  interstices of size  $L_{n-1} L_{n-2}$ :

$$A_{n-2} \sim 2^{-1/2} L_1^2, \quad (16)$$

$$t_{n-2} \sim 2 t_{n-1}. \quad (17)$$

Each population of like interstices contributes the same area ( $\sim 2^{-1/2} L_1^2$ ) to the diffusion coverage of the square, and each such contribution comes in a sequence of doubling time intervals. This sequence is represented by the construction shown in the lower right of Fig. 3. Above  $t/t_n = 1$ , the points fall on a curve  $A(t)$  that has a monotonically decreasing slope. This curve is analogous to the consolidation curve for line-shaped invasion (Fig. 2).

The number ( $n$ ) of area steps ( $2^{-1/2} L_1^2$ ) made during the consolidation phase is finite because the consolidation area matches the available square territory,

$$n 2^{-1/2} L_1^2 \sim 4L_1^2. \quad (18)$$

This means that  $n$  is of order 5 or 6, and that the complexity of the tree design of Fig. 3 is *finite*. The finite complexity is a consequence of the finiteness of the territory, and the

TABLE I. The scales of the S-curve phenomenon.

	Line invasion	Tree invasion
$t_{in}$	$2 \frac{L_1}{V}$	$3.4 \frac{L_1}{V}$
$A_{in}$	$2^{3/2} \left(\frac{\alpha}{V}\right)^{1/2} L_1^{3/2}$	$30 \left(\frac{\alpha}{V}\right)^{1/2} L_1^{3/2}$
$t_{co}$	$\frac{L_1^2}{\alpha}$	$\frac{L_1^2}{5\alpha}$

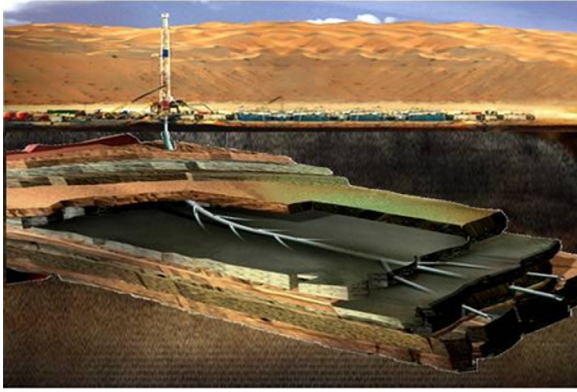


FIG. 4. (Color online) The evolution of human-made volume-point flow underground: drilling and oil extraction pattern under the Empty Quarter, Saudi Arabia (Courtesy of Aramco). This tree-shaped design is an icon of all mining that occurs worldwide: coal, gas, metals, etc.

required transition from diffusion by invasion (convection) to transversal diffusion during consolidation. The total duration of the consolidation phase is

$$t_{co} \sim n t_n \sim \frac{L_1^2}{5\alpha}. \quad (19)$$

This is the lifetime of diffusion spreading by tree invasion and consolidation, and it is significantly shorter than the time scale of line invasion and consolidation (Sec. II), which is  $L_1^2/\alpha$ .

#### IV. THE UNIVERSALITY OF THE S CURVE AND THE HUBBERT PEAK: SPREADING AND COLLECTING FLOWS

The S curve is predicted completely for two invasion scenarios (line, tree), Figs. 2 and 3. The S shapes depend on a single dimensionless group:  $L_1V/\alpha$ . Table I summarizes the quantitative differences between the scales of the two invasion geometries. The tree-shaped design offers a shorter lifetime ( $t_{co}$ ) and a ten times larger diffused territory ( $A_{in}$ ) at the end of the invasion phase.

The inflection of the S curve is located at  $t \sim t_{in}$  and  $A \sim A_{in}$ . This is a key feature because it represents the time of the maximum rate of diffused area increase  $dA/dt$ , i.e., the maximum rate of spreading.

All these predictions apply equally to the behavior of collecting flows, which extract mass or energy from areas or volumes and carry them to discrete points. For collecting flows, the scales of the S inflection ( $t_{in}$ ,  $A_{in}$ ) indicate the all-important regime of peak production rate, known as the “Hubbert peak” in oil extraction.<sup>22–24</sup> It is not a coincidence

that oil extraction technology has evolved from single-line invasion (the single well) to tree invasion, e.g., Fig. 4.

The S-curve phenomenon and its configuration principle unite the spreading flows with the collecting flows, and the animate flows with the inanimate flows. In the human realm, they unite the designs for urban infrastructure with the underground architectures for mining (coal, metals, heat from the ground), and teach the physics of “limits to growth” and when a spreading population and technology can be expected to “hit the wall.” (e.g., fossil resources, water, economic bubble, boom and bust, pyramid scheme) They also cover the periodic phenomena of spreading and collecting, such as respiration (inhaling, exhaling),<sup>11,25,26</sup> drug delivery, excretion, rain water (from river basin to delta), and blood circulation. All these domains deserve renewed theoretical investigation in view of the constructal design disclosed in this paper.

#### ACKNOWLEDGMENTS

This research was supported by grants from the National Science Foundation, the U.S. Air Force Office of Scientific Research, and the National Renewable Energy Laboratory.

<sup>1</sup>R. Pearl, *Q. Rev. Biol.* **51**, 6–24 (1976).

<sup>2</sup>W. Easterly, *The White Man's Burden* (Penguin Books, London, 2006).

<sup>3</sup>A. Bejan, *Int. J. Heat Mass Transfer* **40**, 799 (1996).

<sup>4</sup>J. W. Lu and P. W. Beamish, *The Acad. Manage. J.* **47**, 598 (2004).

<sup>5</sup>M. Nishioka, C. K. Law, and T. Takeno, *Combust. Flame* **104**, 328 (1996).

<sup>6</sup>P. Asthana, *IEEE Spectrum* **32**, 49 (1995).

<sup>7</sup>S. E. Kingsland, *Modeling Nature: Episodes in the History of Population Ecology* (University of Chicago Press, Chicago, 1995).

<sup>8</sup>A. Grübler, *The Rise and Fall of Infrastructures: Dynamics of Evolution and Technological Change in Transport* (Physica, Heidelberg, 1990).

<sup>9</sup>A. Bejan and S. Lorente, *Philos. Trans. R. Soc. London, Ser. B* **365**, 1335 (2010).

<sup>10</sup>A. Bejan and S. Lorente, *J. Appl. Phys.* **100**, 041301 (2006).

<sup>11</sup>A. Bejan, *Advanced Engineering Thermodynamics*, 2nd ed. (Wiley, New York, 1997), p. 807.

<sup>12</sup>A. H. Reis, *Appl. Mech. Rev.* **59**, 269 (2006).

<sup>13</sup>A. F. Miguel, *J. Theor. Biol.* **242**, 954 (2006).

<sup>14</sup>H. Poirier, *Sci. Vie* **1034**, 44 (2003).

<sup>15</sup>W. Wechsattel, J. C. Ordonez and S. Kosaraju, *J. Appl. Phys.* **100**, 113514 (2006).

<sup>16</sup>S. Quéré, *Int. J. Des. Nat. Ecodyn.* **5**, 242 (2010).

<sup>17</sup>J. Lewins, *Int. J. Heat Mass Transfer* **46**, 1541 (2003).

<sup>18</sup>X. Daguene-Frick, J. Bonjour, and R. Revellin, *IEEE Trans. Compon. Packag. Technol.* **33**, 115 (2010).

<sup>19</sup>J. Fan and L. Wang, *Int. J. Heat Mass Transfer* **53**, 4238 (2010).

<sup>20</sup>G. Weinerth, *Int. J. Des. Nat. Ecodyn.* **5**, 268 (2010).

<sup>21</sup>A. Bejan, *Convection Heat Transfer*, 3rd ed. (Wiley, Hoboken, NJ, 2004).

<sup>22</sup>M. K. Hubbert, *Science* **109**, 103 (1949).

<sup>23</sup>A. R. Brandt, *Energy Policy* **35**, 3074 (2007).

<sup>24</sup>T. W. Patzek and G. D. Croft, *Energy* **35**, 3109 (2010).

<sup>25</sup>E. R. Weibel, *Symmorphosis: On Form and Function in Shaping Life* (Harvard University Press, Harvard, 2000).

<sup>26</sup>H. Hoppeler and E. R. Weibel, *J. Exp. Biol.* **208**, 1573 (2005).